Nearshore Side-Scan Sonar Studies

S. A. THORPE

Department of Oceanography, The University, Southampton, United Kingdom

A. J. HALL

Institute of Oceanographic Sciences, Wormley, Godalming, Surrey, United Kingdom

18 September 1992 and 24 March 1993

ABSTRACT

Side-scan sonars operating at 80–250 kHz have been deployed to produce narrow beams directed parallel and normal to shore on a gently sloping beach. These provide measurements of processes (such as wave propagation) seaward of the edge of the surf zone. Shoreward propagation of sound into the surf zone and hence useful information retrieval from this zone is prevented, however, by high bubble or suspended sediment absorption at its outer edge, as found in earlier Doppler sonar studies at 195 kHz by J. A. Smith. The shoreward limit of acoustic propagation has a variable structure related to incident wave groups, the position at which waves break, and to dynamical processes within the surf zone determining the position of the bubble or suspended sediment boundary.

1. Introduction

Smith (1993) has described the novel use of surface-scanning 195-kHz Doppler sonar as a tool to investigate nearshore processes. He finds no degradation of signal due to multiple surface or bottom reflections but observes that extremely dense bubble clouds formed by plunging breakers produce an impenetrable "wall" at the breakpoint, where sound is severely attenuated. Useful measurements of reflected sound intensity and velocity are obtainable only seaward of the breakpoint.

We have used side-scan sonars directed from deep water toward shore, together with sonars directed parallel to shore, on a smooth east-facing beach extending for 3 km to the north and some 30 km to the south of the observation site, in the North Sea on the coast of England. The sonars can detect signals reflected from waves approaching the surf zone and from scatterers, such as isolated bubble clouds, in the water column, which provide information about the nearshore dynamics. Examples are given in section 2. At the sonar frequencies used here, 90–250 kHz, sound propagation into the surf zone is prevented by severe attenuation, as found by Smith at 195 kHz. The limit of sonar range is often clearly marked as a narrow region of high target strength but has a variable structure.

Corresponding author address: Dr. S. A. Thorpe, Department of Oceanography, The University, Southampton, SO9 5NH, United Kingdom.

2. The sonars

A weighted rig carrying four sonar transducers at a height of 0.55 m was placed on a smooth 1° sloping sandy beach at low tide and connected to recording instruments contained in a van by 200 m of cable buried in the sand for protection (Fig. 1). The M2-dominated tidal range at the rig was about 3.2 m. The rig maintained its orientation and setting to better than 4° over the 5-day experiment. The linear sonar transducers were set to point horizontally. Once covered by the rising tide, they produced beams 46° (80- and 90-kHz sonars) and 30° (250-kHz sonars) wide in the vertical and 2° wide in the horizontal (all sonars; beam angles measured to the −3-dB points), so isonofying narrow vertical sections of water, typically 1–3 m wide. A 90- and a 250-kHz sonar were directed to point directly up the beach (in direction 270°), and an 80- and a 250-kHz sonar pointed parallel to the shoreline (direction 180°). The sonars were operated in pulsed mode with repetition rates set to 5, 6, or 8 Hz, for 8–10 h on each of seven tides. The pulse lengths were 0.14 ms for the 80- and 90-kHz sonars and 0.096 ms for the 250-kHz sonars, giving range resolutions of about 0.2 and 0.14 m, respectively. Although the 250-kHz sonars did have slightly better resolution, comparisons with the two other frequencies showed little qualitative improvement in the sonograph records, and in general no greater ranges were obtained, and for simplicity we shall confine the later examples to the records produced at the lower frequencies. The 80- and

© 1993 American Meteorological Society

Unauthenticated | Downloaded 08/07/24 03:50 AM UTC

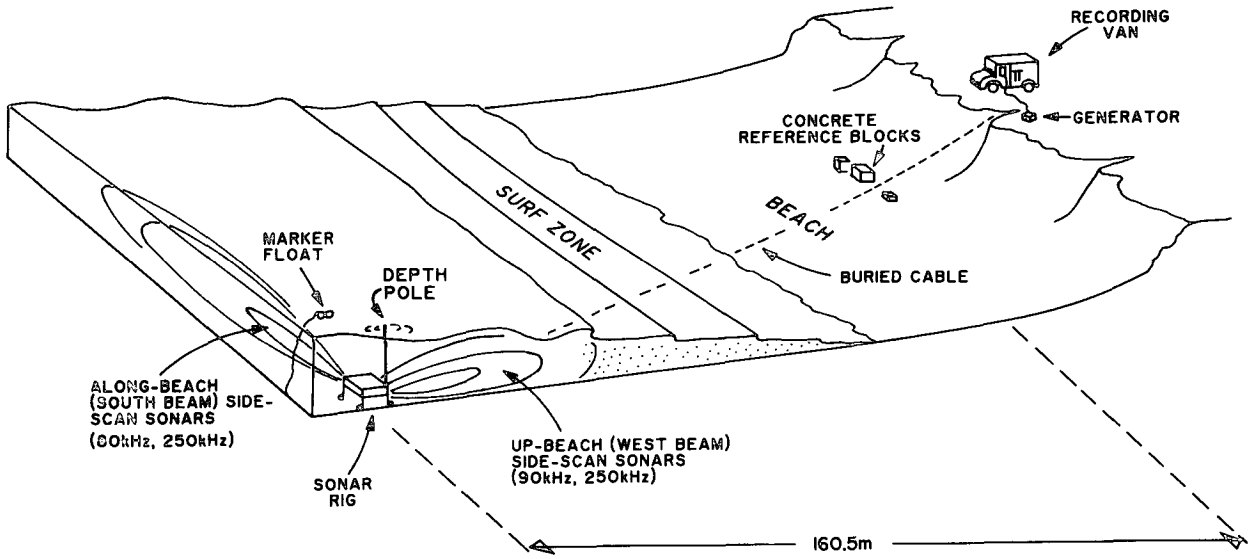

FIG. 1. Sketch of the site and sonar configuration.

90-kHz sonars were driven and received remotely via the cable. The transmission frequency was heterodyned directly down to 10 kHz with a ±5-kHz bandwidth. In situ electronics were used to adjust the 250-kHz transducers. A heterodyned frequency of 36 kHz was used to transmit the signal along the cable where it was also mixed down to 10 kHz. Two channels of sonar data were sampled at 44.1 kHz (frequency response 10–20 kHz, 90-dB dynamic range) by a Sony PCM 701ES digital audio processor and recorded on the video channels of an AKAI VS-512 EK VCR. The hi-fi channels of the VCR were used to record further channels in analog format. Sonographs from any two of the sonars could also be produced in real time on a Waverley thermal line-scan recorder. Examples are shown in later figures. The 80- and 90-kHz sonars had a 20-ms "defended" zone following the trigger pulse, and signals from ranges less than about 15 m (0.5 × 20 ms × sound speed) were therefore lost.

3. The observations

Figure 2 is an example of a sonograph record (range versus time) obtained using the two lower-frequency transducers in winds of 11 m s^{-1} (gusting to 14 m s^{-1}) blowing from direction 180°, parallel to shore. Waves could be seen approaching shore from about 145° with a period estimated as 3.7 s and a height of 0.4–0.7 m at the edge of the surf zone. The water depth at the sonar was 1.9 m. The upper record is from the 80-kHz transducer directed parallel to shore and shows streaks (e.g., *AA*) with low slopes representing targets moving northward toward the sonar (range decreasing with time) at speeds of 13 ± 1 cm s^{-1}. Occasionally the origin of these streaks was visible as a dark, well-defined,

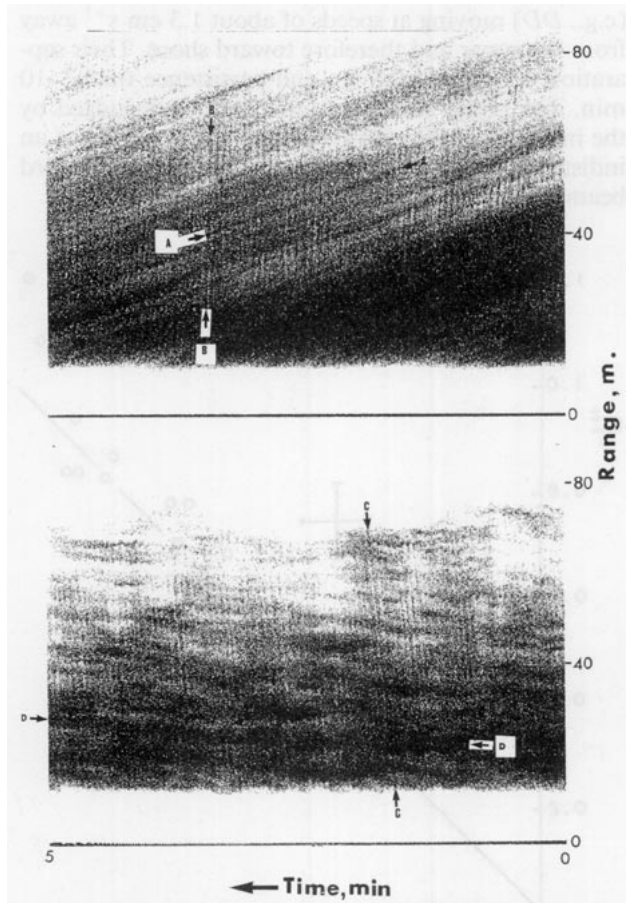

FIG. 2. Sonograph record, range versus time, with (above) 80-kHz parallel-to-shore sonar and (below) 90-kHz shoreward-pointing sonar. The darker the record, the greater is the strength of the scatterers. A period of 5 min is shown; time increases to the left. Water depth at sonar is 1.9 m. Features *AA*, etc., explained in text, are best seen by viewing along the line of the arrows.

Unauthenticated | Downloaded 08/07/24 03:50 AM UTC

and strongly reflecting target, which earlier studies (e.g., Thorpe and Hall 1983; Thorpe 1992; Osborn et al. 1993) have identified as breaking waves. These streaks are the advected motion of the wave-produced bubble clouds, which form strong acoustic targets and persist for 2–5 min and which are advected down the sonar beam by an alongshore current. The streaks therefore provide a measure of the alongshore component of the current resulting from a northerly tidal component, together with wave and wind-induced drift, near and in the water depth of the sonar rig. Smaller-scale, regularly spaced lines (e.g., *BB*) appear to approach the sonar at speeds of 6.4 ± 0.4 m s^{-1}. These have lengths of up to 60 m and periods of 3.5 ± 0.3 s. Their wavelength in the beam direction, parallel to shore, is 23 ± 4 m. Similar lines, moving away from the sonar are visible in the 90 kHz, shoreward-pointing beam shown in the lower part of Fig. 2 (e.g., *CC*). These lines have the same period but their tilt at short range in the range–time plot implies a speed toward shore of 5.1 ± 0.4 m s^{-1} near the sonar and an onshore wavelength of 18 ± 3 m. The 90-kHz record also shows banded targets (e.g., *DD*) moving at speeds of about 1.3 cm s^{-1} away from the sonar and therefore toward shore. Their separation is typically 5–7 m, and persistence time 5–10 min. The target strength in this record, as judged by the intensity of the record, falls off with range, but an indistinct "edge" is sometimes visible in the shoreward beam at about 75 ± 10 m.

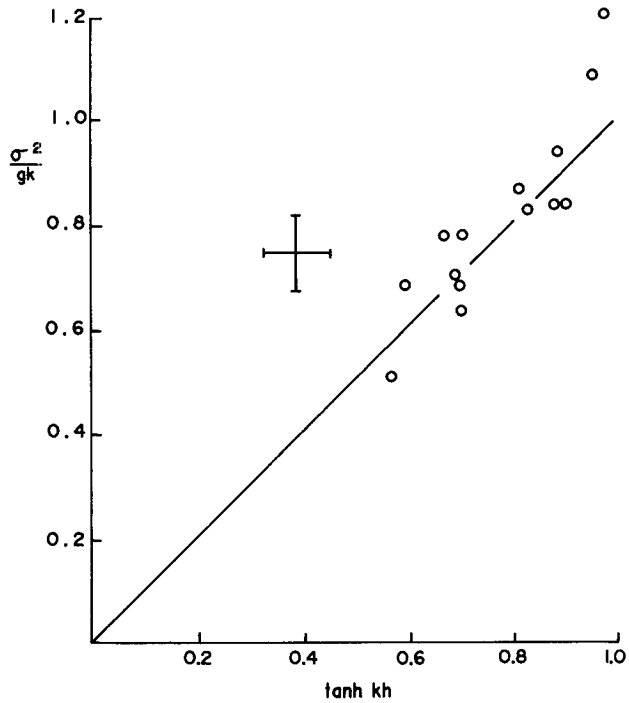

FIG. 3. Test of the linear dispersion relation. The cross shows the magnitude of the errors in estimating the points, obtained from sonar data at different times.

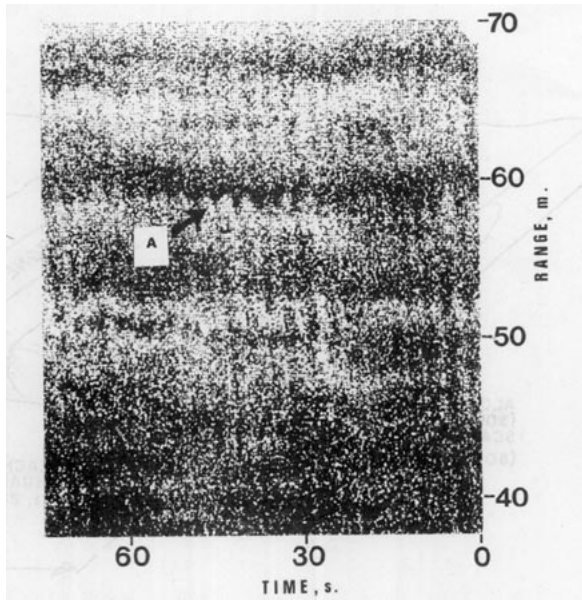

FIG. 4. Sonograph of the 90-kHz shoreward-pointing sonar, showing at *A* the horizontal displacements of bubble clouds as waves propagate past them. The record was obtained 30 min after Fig. 2. The water depth at a range of 60 m from the sonar, near the scattering band marked *A*, is 0.9 m.

The higher-frequency lines with periods of about 3.5 s are identified as being progressive surface waves moving toward shore from a direction, determined from the relative apparent speeds of the lines in the two beams, of $140° \pm 10°$. The features are consistent with the linear dispersion relation of waves in water of finite depth,

$$\sigma^2 = gk \tanh(kh), \qquad (1)$$

where σ is the wave frequency, g the acceleration due to gravity, k the wavenumber derivable from the two component wavelengths, and h the water depth; the plot of σ^2/gk against $\tanh(kh)$ shown in Fig. 3 is approximately linear. An objective technique using the digitized data has been developed by Crawford (1992) to measure the speed of the sonar wave bands and this confirms that, within the error bars of Fig. 3, they conform to linear theory.

The 90-kHz sonographs show that, where the surface wave lines intersect well-defined edges of the banded targets like those at *DD* in Fig. 2, the latter are displaced toward the sonar; between the wave lines the displacement is toward shore. This is shown in Fig. 4. The total displacement here is 1.4 ± 0.2 m. The pattern is asymmetrical, a rapid offshore rate of displacement being followed by onshore motion of similar or greater magnitude and then a period of relatively little displacement before the cycle restarts, characteristic of waves approaching breaking. The development of a similar asymmetry in the velocity field as waves approach shore has been noticed in Smith's Doppler re-

Unauthenticated | Downloaded 08/07/24 03:50 AM UTC

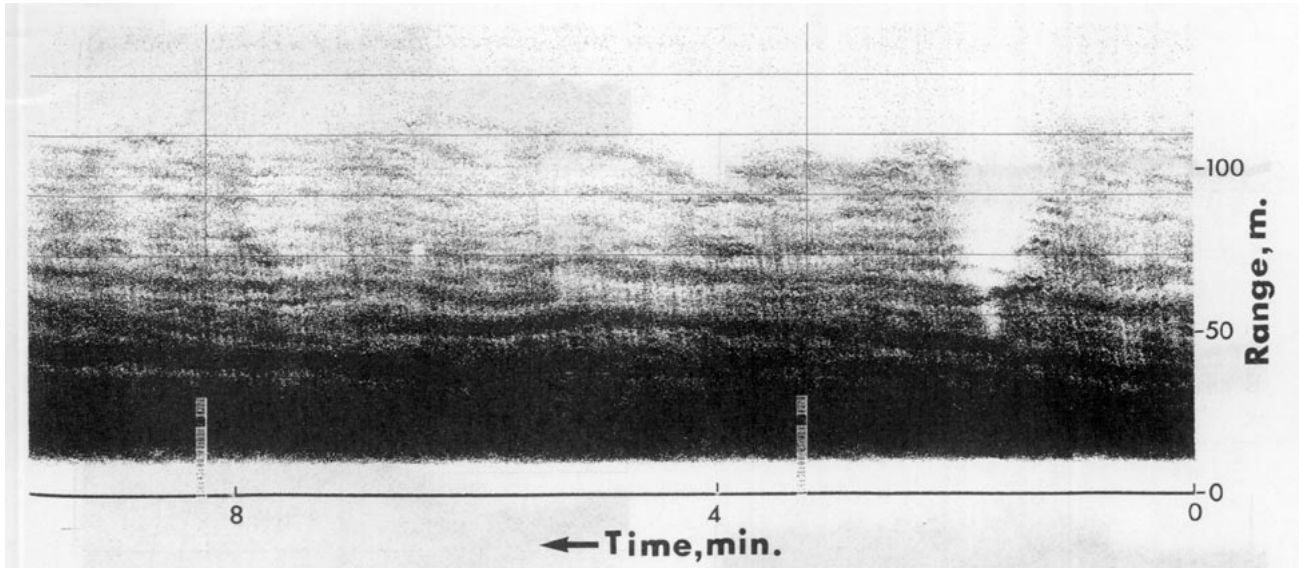

FIG. 5. Sonograph of the 90-kHz shoreward-pointing sonar showing continuous bands of bubbles. The bands are best seen by viewing the sonograph from a low angle at one end. The alongshore 3-min average drift estimated from 80-kHz sonar is 36 ± 2 cm s^{-1} to the north. The vertical lines are 5 min apart. A reduction in sonar range occurs at about 1 min after the start of the record. Wind speed is 10–14 m s^{-2} from 230°. Dominant waves approached the sonar from 140°.

cords (1992, private communication). The phase of the motion implies that the wave lines are themselves associated with times of little, or no, onshore motion but high onshore acceleration. This identifies the source of the wave lines as being caused by sound scattering from the leading face of waves as they approach shore, between the offshore flow near the wave trough and the onshore flow at the crest. The amplitude of the observed displacements is found to be consistent with the mean depth-integrated horizontal displacements, $x = (2ac/h)\cos\alpha$, produced by progressive waves, estimated as 1.5 ± 0.5 m. Here $c = \sigma/k$ is the wave phase speed, $2a$ is the wave height, α is the angle of the wave crest to the shoreline, and h is the water depth, all estimated from the sonar records and beach survey at the position of the displaced band in Fig. 4.

The separation and persistence of the banded targets (*DD*, Fig. 2) seen in the 90-kHz records are consistent with their being caused by Langmuir circulation, creating bands of sound-scattering bubble clouds roughly parallel to the wind direction (see Thorpe 1984; Zedel and Farmer 1991). A further example is shown in Fig. 5. The persistence time of 5–10 min in the alongshore current of 13 cm s^{-1} in Fig. 2 (or 36 cm s^{-1} measured by the 80-kHz sonar at the time the Fig. 5 record was obtained) implies lengths of 40–200 m, or 7–12 times the separation between neighboring bands.

The maximum achievable range in both 90- and 250-kHz shoreward-pointing sonars was restricted, being usually less than the ranges of 150 m obtained in water 30 m deep (Thorpe and Hall 1983). Figure 6 shows this range plotted against the distance from the sonar to the outer edge of the surf zone estimated by observers. While there is considerable uncertainty in the latter, the correspondence in the two estimates is consistent with Smith's (1993) conclusion that the sonar range is limited to the outer edge of the surf zone

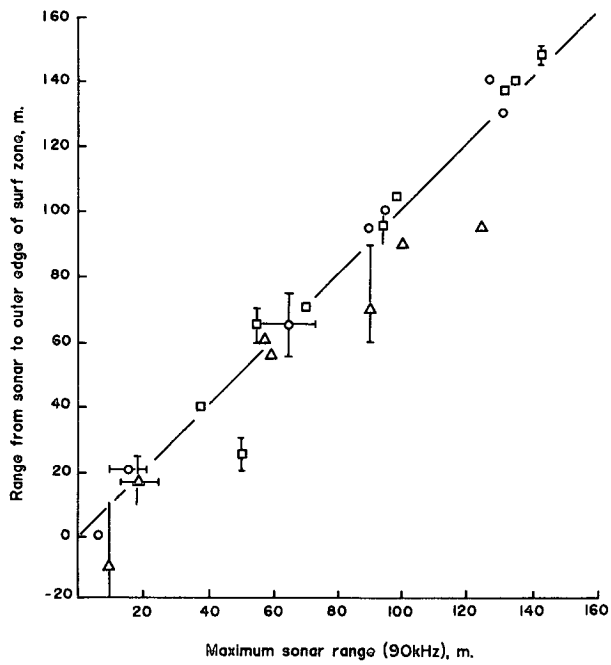

FIG. 6. The variation in range of the edge of the surf zone, as judged by visual observations, versus the maximum range obtained by the shoreward-pointing sonars. Different symbols are used for observations on different tides. Bars indicate the uncertainty in the estimates.

Unauthenticated | Downloaded 08/07/24 03:50 AM UTC

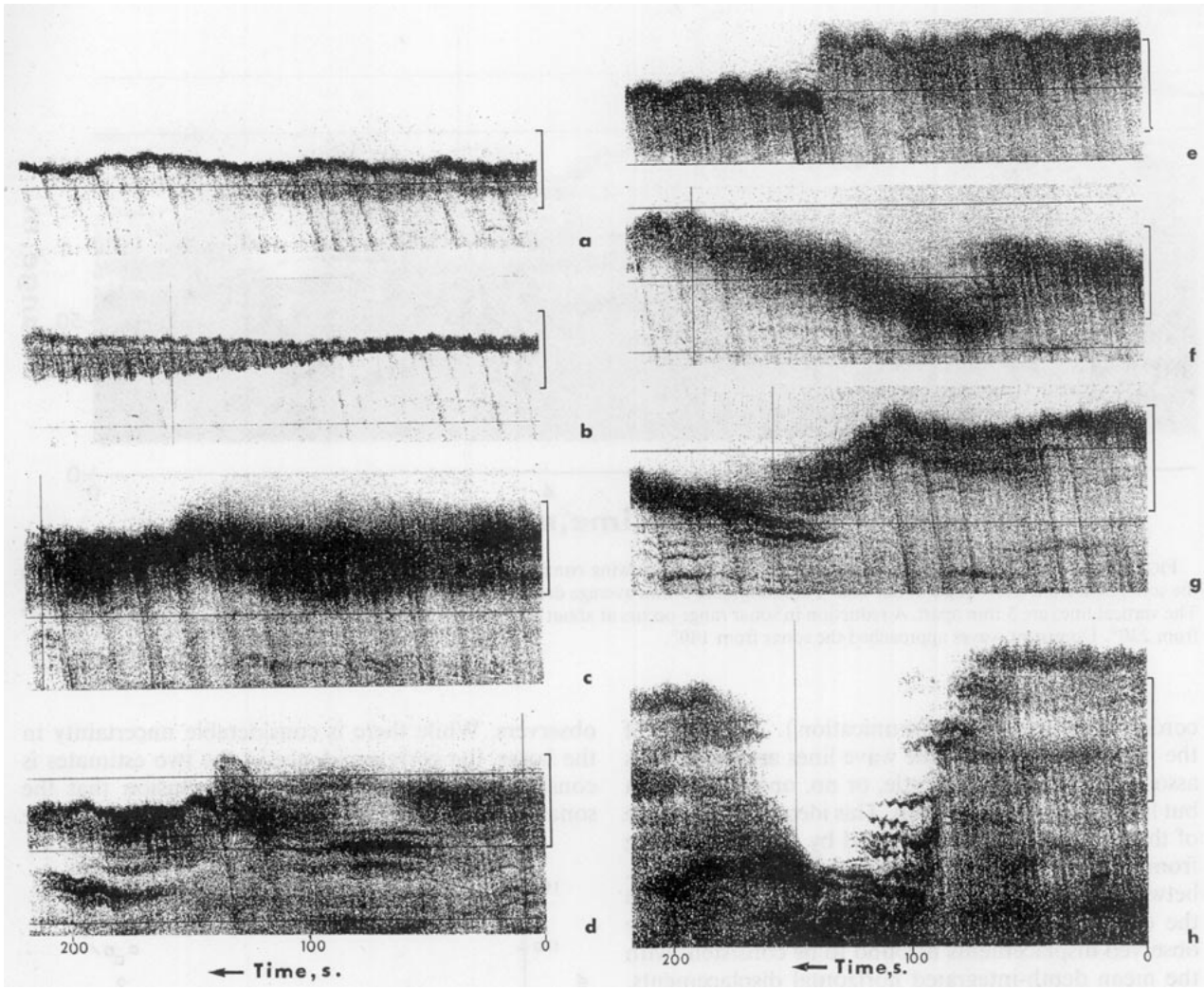

FIG. 7. Sonographs from the 90-kHz sonar, showing the highly variable structures observed near the shoreward limit of sonar range. Each record is 218 s in length, time increasing to the left, and the vertical bars indicate 20 m of range. (a) A continuous narrow region of high scattering with evidence of some reduction in range where strongly scattering waves reach the sonar limit; wind speed is 3 m s^{-1} from 240°. (b) A splitting of the boundary leading to (c), a broad diffuse scattering region. [Same wind as in (a). The mean water depth at the limit of sonar range is 1.0 ± 0.2 m in (a)–(c). Dominant waves were approaching the sonar from 100°.] (d) A sonar range boundary responding to the arrival of individual waves and wave groups, one of which results in an increase of range followed by abrupt reduction. (e) Periodic structure associated with wave groups, with an abrupt reduction in range where a wave breaks, producing sound-attenuating bubbles. (f) A broad diffuse region as in (c) but with eddylike structure. (g) Gradual reduction in range possibly associated with breaking waves. [Panels (d)–(g) have the same wind conditions, 8 ± 2 m s^{-1} from 235°. The mean water depth at the edge of sonar range is 0.8 ± 0.2 m.] (h) Wave breaking resulting in a large reduction in range, possibly resulting from bubbles and sediment attenuation. Wind speed is 8 m s^{-1} from 180°. Dominant waves approaching the sonar from 138°.

at 195 kHz, and also suggests it is true at 90 and 250 kHz. Although Figs. 2 and 5 provide examples in which the outer limit of sonar range is indistinct, often the limit was well defined and marked by a strongly reflecting band but with considerable variability in structure, as illustrated in Fig. 7. Figure 7a shows a record with a band of enhanced scattering near the limit of sonar range, which, in Fig. 7b, splits, creating a broad scattering zone (Fig. 7c). The edge of range in Fig. 7a and shorter-range targets at the left of Fig. 7c are modulated by wave groups marked by one- or two-wave strongly scattering wave lines, over a time corresponding to that of four to six wave periods. These wave group–related features are also seen in Figs. 7d,e, which include an abrupt reduction in range of some 10 m, similar to that shown by Smith (his Fig. 13). An eddylike structure is visible in Fig. 7f. Figure 7g has a reduction in range of some 10 m associated with fine bands of scatterers, presumably bubble clouds from breaking waves, while in Fig. 7h the range is abruptly reduced by about 35 m. This was the largest nontidal change observed. Sound attenuation is preceded by the

Unauthenticated | Downloaded 08/07/24 03:50 AM UTC

appearance of dark filamentary bands of intense scattering emanating from surface wave lines. The filaments appear sequentially. The first to appear are farthest from the sonar. Subsequent filaments appear from later wave lines, closer to the sonar and some 4–5 m farther offshore. The filaments, interpreted as bubble clouds produced by the breaking waves, are themselves advected on- and offshore by subsequent waves, but their mean range changes very little, suggesting that in this case the cause of the reduction in range is not a strong offshore advection of surf-zone bubbles or sediment by a rip current, for example. [The beach is locally regarded as safe for bathing with no history of rip currents. Smith (1992), however, has found evidence of the presence of rip currents in his data.] The feature in Fig. 7h is a consequence of a group of waves breaking prematurely beyond the mean location of the outer edge of the surf zone, the bubbles created and sediment scoured from the seabed possibly contributing to the attenuation. The mean fall speed of the sand grains composing the sediment was about 3 cm s^{-1} leading to their removal from the water column in about 45 s. This is roughly the duration of the attenuation event. There is some indication that bubble clouds created before the event outlive it and persist after the initial range (here 60–70 m) is almost reestablished. The dynamical difference between this "event" and that shown in Fig. 7e is, however, unclear.

An unknown, but important, factor in interpreting the sonograph data, particularly the offshore movements of acoustic targets, is the vertical distribution of bubble scatters in the water column and their associated scattering cross section per unit volume at the sonar frequencies. This has yet to be measured in the nearshore zone. In deep water the mean scattering cross section decays vertically as depth increases, in an approximately exponential way on a scale of 0.65–2.27 m (Thorpe 1986); scattering will, however, extend deeper close to breaking waves and in the convergence zones of Langmuir circulation (Thorpe 1984). In the highly turbulent region of repetitive wave breaking in the relatively shallow (here 0.8–1.0 m) water at the edge of the surf zone, the mean vertical distribution of bubbles resonant at the sonar frequencies, 15–50 μm, may, in comparison to deep water, be relatively uniform.

4. Conclusions

We have provided, in this note, a few examples that illustrate the potential of side-scan sonar at 80–250 kHz as a means to study processes in the coastal zone. As found by Smith (1993) using a 195-kHz Dopper sonar, the useful onshore range is limited by sound attenuation near the outer edge of the surf zone caused, presumably, by bubbles and suspended sediment. The limit of range is sometimes clearly marked by a band of intense scatterers but of variable form (Fig. 7), and more research is needed to establish the physical nature of this band and its variability in response to incident waves and surf-zone dynamics.

Acknowledgments. The sonar observations were made with support from the ONR under Grant N00014-92-3-1288. Able assistance in the collection of data was provided by M. Cure, A. R. Crawford, and J. Jackson. SAT is grateful to the MPL, Scripps Institution of Oceanography, for providing facilities during his study leave visit in September 1992, and particularly to Dr. J. Smith for showing his paper prior to publication and for stimulating discussions about his data.

REFERENCES

Crawford, A. R., 1992: An evaluation of side-scan sonar as a tool to study the near-coastal zone. M.S. dissertation, University of Southampton, 50 pp.

Osborne, T., D. M. Farmer, S. Vagle, S. A. Thorpe, and M. Curé, 1993: Measurements of bubble plumes and turbulence from a submarine. *Atmos.-Ocean,* **30,** 419–440.

Smith, J. A., 1992: Nearshore observations with a surface-scanning Doppler sonar. *EOS,* **72**(Suppl), 256.

——, 1993: Performance of a horizontally scanning Doppler sonar near shore. *J. Atmos. Oceanic Technol.,* **10,** 752–763.

Thorpe, S. A., 1984: The effect of Langmuir circulation on the distribution of bubbles caused by breaking waves. *J. Fluid Mech.,* **142,** 151–170.

——, 1986: Measurements with an automatically recording inverted echo sounder: ARIES and the bubble clouds. *J. Phys. Oceanogr.,* **16,** 1462–1478.

——, 1992: Bubble clouds and the dynamics of the upper ocean. *Quart. J. Roy. Meteor Soc.,* **118,** 1–22.

——, and A. J. Hall, 1983: The characteristics of breaking waves, bubble clouds and near-surface currents observed using side-scan sonar. *Contin. Shelf Res.,* **1,** 353–384.

Zedel, L., and D. M. Farmer, 1991: Organised structures in subsurface bubble clouds: Langmuir circulation in the open sea. *J. Geophys. Res.,* **96,** 8889–8900.

Unauthenticated | Downloaded 08/07/24 03:50 AM UTC